Smoothing CRS Attributes for Processing and Imaging

Fernando S. M. Nunes, Lourenildo W. B. Leite, UFPA, Brazil

Abstract

We examined in this work the effect of smoothing the CRS (comum reflector surface) attributes in the process of stack and migration. Tests were performed on synthetic data (Marmousoft), and the workflow that generated the best results was used for processing the marine real data (Jequitinhonha). As result, the CRS migration section showed sensitivity to the smoothing process, that can be considered to become part of the workflow for niptomography as well.

Introduction

The specific aim of this work was to examine how the smoothing process of the CRS attributes influence the results of the CRS stack and migration. Several tests were performed on synthetic data, and some modifications were observed in the results with emphasis to the CRS migration sections that showed better improvement in the signal/noise ratio in the complex regions. Theorectically, it is desired to jump out of any local minimum, searching for the global minimum of the object semblance function, and here we investigate on the possibility of using a smoothing process previous to the final optimization.

The workflow that generated better results on synthetic data was used on line L2140270 of the Jequitinhonha Basin, which has potential for petroleum exploration (Mohriak et al., 2008).

CRS Stack and Migration

The CRS stack is based on a layered model with curved interfaces as reflectors, where the hyperbolic operator of primary reflections in the neighborhood of a normal central ray given by:

$$t_{hip}^2(x_m,h) = \left[t_0 + 2\frac{\sin\beta_0}{v_0}(x_m - x_0)\right]^2 +$$

$$+2t_0\frac{\cos^2\beta_0}{v_0}\left[\frac{(x_m-x_0)^2}{R_N} + \frac{h^2}{R_{NIP}}\right]; \qquad (1)$$

where v_0 is the layer velocity near to the emergence point $P_0(x_0,t_0)$, t_0 the two-way time of a ray that simulates a normal trajectory, x_m the mid point coordinate, h the half offset coordinate, and x_0 the spatial coordinates of the reference point $P_0(x_0,t_0)$, t_0 (Mann et al., 2003). The CRS operator is defined as independent of a velocity model, and (R_{NIP}, R_N, β_0) are the parameters that define the stack surface (Muller, 1999).

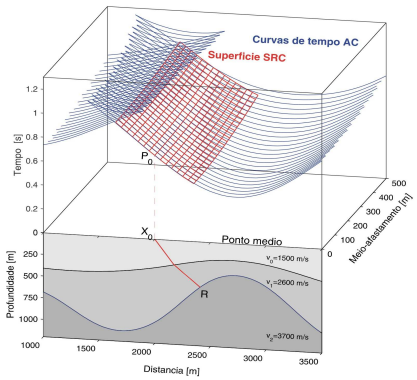

Figure 1: (Lower part) Model composed of two layers over a half-space. The normal ray has red color. (Upper part) The blue surface is related to the CRS stack corresponding to the reflection point R calculated by the hyperbolic approximation given by equation (1).

These three attributes are obtained as a solution of non-linear optimization problems, where the object of minimization is the semblance function. To initialize the attribute search, equation (1) is simplified for specific cases. In the first step, it is set $x_m = x_0$, which simplifies equation (1) as a CMP (comum medium point) operator with the parameter as a combination of the form $q = \frac{\cos^2\beta_0}{R_{NIP}}$. In the second step, it is set $h = 0$, which provides an operator in ZO (zero-offset) configuration. Considering a first order approximation, β_0 is calculated, and with a second order approximation R_N is calculated, and next R_{NIP} is calculated through the combination of q. These initial steps result in (β_0^{ini}, R_{NIP}^{ini}, R_N^{ini}). The next step is the optimization using the Simplex method (Mann, 2002). Figure 1 shows the surface of the data and of the CRS operator that are adjusted during the search process.

For CRS migration, the Kirchhoff operator, $t_D(x_m,h)$, based on the attributes (R_{NIP}, R_N, β_0) is a special case of the CRS operator given by equation (1) where $R_{NIP} = R_N$ (Mann, 2002):

$$t_D^2(x_m,h) = \left[t_0 + 2\frac{\sin\beta_0}{v_0}(x_m - x_0)\right]^2 +$$

$$+2t_0\frac{\cos^2\beta_0}{v_0 R_{NIP}}\left[(x_m-x_0)^2 + h^2\right]. \qquad (2)$$

The apex of this hyperbolic operator is located at $h = 0$,

and this point is found at $\frac{\partial t_D(x_m,h=0)}{\partial x_m} = 0$ that takes to find the apex coordinates, (x_{ap}, t_{ap}), by the forms:

$$x_{ap} = x_0 - \frac{R_{NIP} t_0 v_0 \sin\beta_0}{2R_{NIP}\sin^2\beta_0 + t_0 v_0 \cos^2\beta_0}; \quad (3)$$

and

$$t_{ap}^2 = \frac{t_0^2 v_0 \cos^2\beta_0}{2R_{NIP}\sin^2\beta_0 + t_0 v_0 \cos^2\beta_0}. \quad (4)$$

The migration operator given by equation (2) depends only on β_0 and R_{NIP} and, therefore, the smoothing process of the R_N is irrelevant to the results of the CRS migration.

For the smoothing process was used the routine *smooth2* of the Seismic Un*x. For the main tests, it was used 5, 10, 15 and 20 points for smoothing, and the results were similar to both data sets. For presentation, the smoothing of the syntetic data was decided for 5 points, and for the real data 10 points due to better visual results.

Results

The main results are the stack and migration sections obtained with the operators given by equations (1) and (2), respectively. These sections were analyzed after the smoothing process as a way to filter attribute noise on the high frequency range.

The main observations of the results are comum to both data sets. In this aspect, the attribute smoothing proved to be effective for the attenuation of high frequency attribute noise; however, the smoothed attribute stack sections were similar to those found before the smoothing process, and the sections that had better results were the migration sections, where was shown a decrease in the noise, and an improvement of visual quality in the complex areas. The basic difference of the stack strategies analyzed in this work are shown in the block diagrams of the figures (2) and (3).

The pre-processing step was not performed on the Marmousoft synthetic data, and began directely with the CRS stack according to the block diagram of figure 2 followed by figure 3. It was clear that the smoothing process was able to diminish some random noise present in the attributes, that can be verified by comparing sections of the figures 4, 5 and 6. The stack sections of the figure 7 do not show a major difference between them, but the smoothing process improved the visual quality as shown in figure 8, specially in the marked areas where structures show better continuity. This same strategy was used for the processing of the Jequitinhonha data.

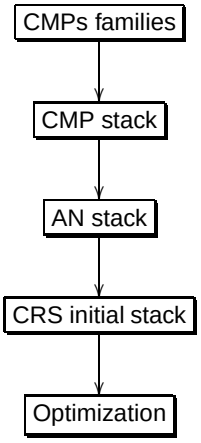

Figure 2: Block diagrams of the CRS stack.

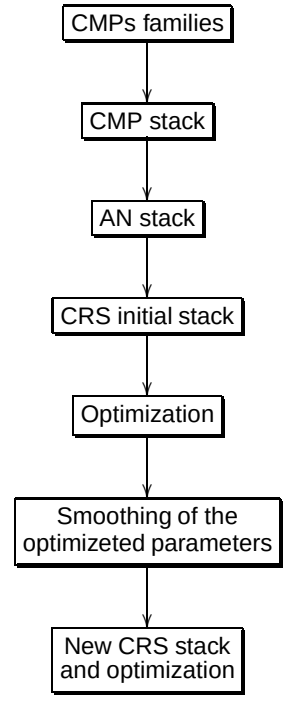

Figure 3: Block diagrams of the CRS stack with smoothing attribute process.

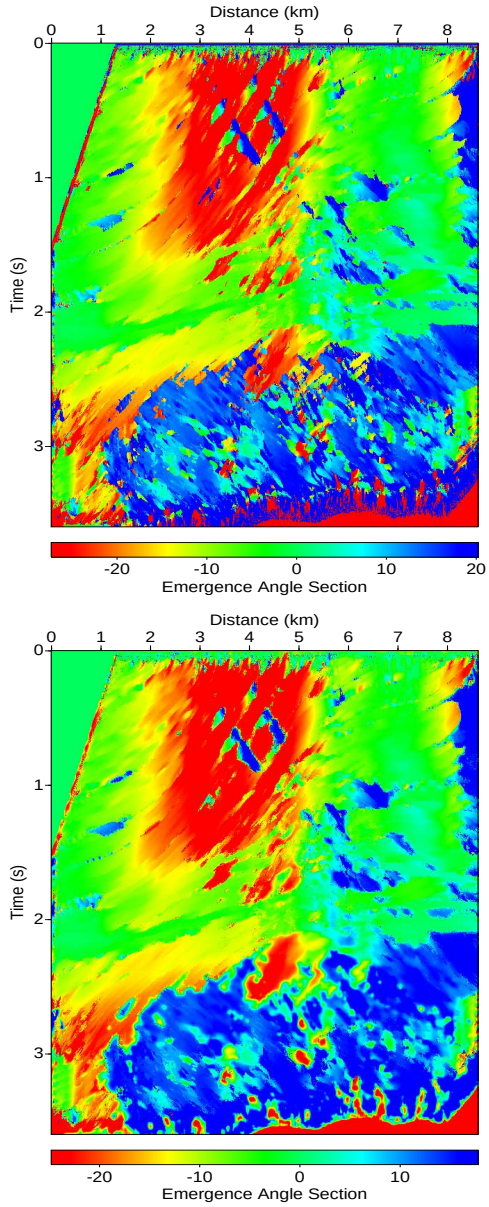

Figure 4: Emergence angle section β_0 before (above) and after (below) attribute smoothing with 5 points. In both sections it is seen the structural features, but with the smoothing it is possible to observe these structures with better signal/noise ratio.

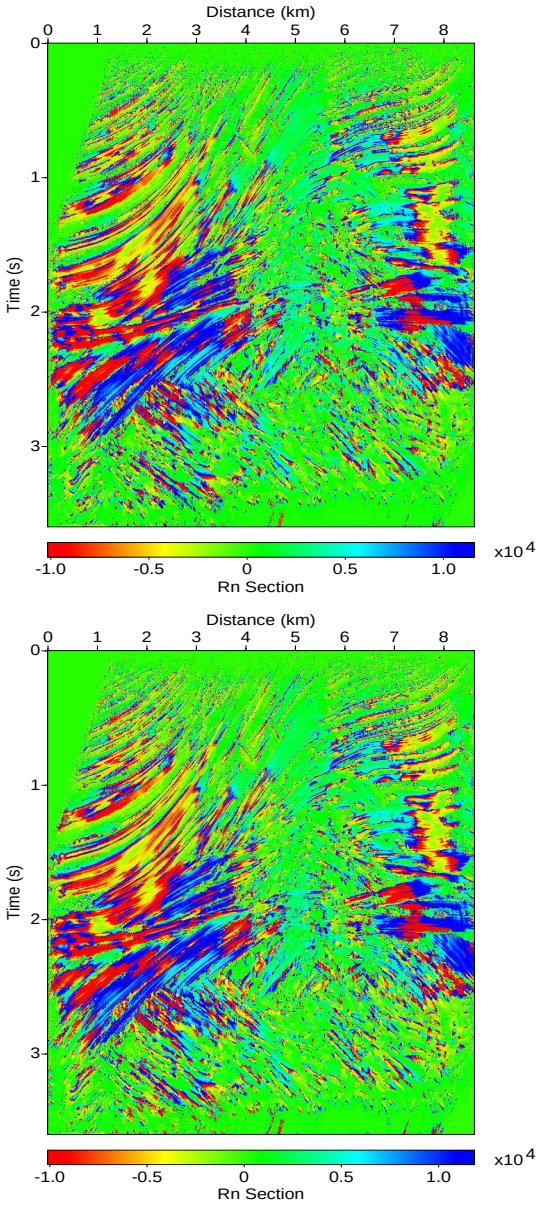

Figure 5: Curvature ray section R_N before (above) and after (below) attribute smoothing with 5 points. In both sections it is seen the structural features, but with the smoothing it is not possible to observe these structures with big changes in the signal/noise ratio.

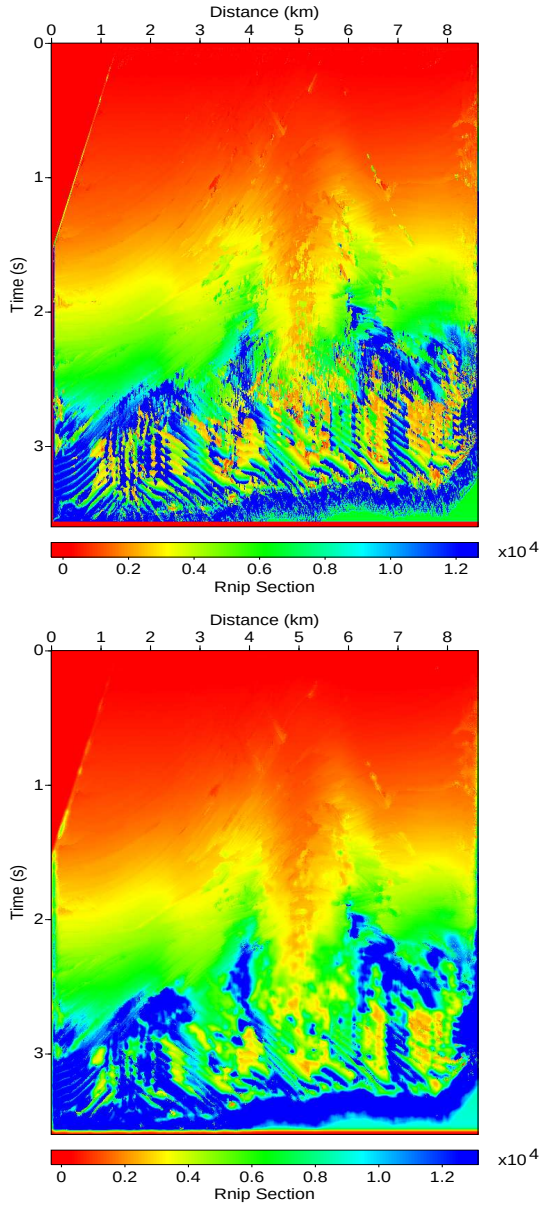

Figure 6: Curvature ray section R_{NIP} before (above) and after (below) attribute smoothing with 5 points. In both sections it is seen the structural features, but with the smoothing it is possible to observe these structures with better signal/noise ratio.

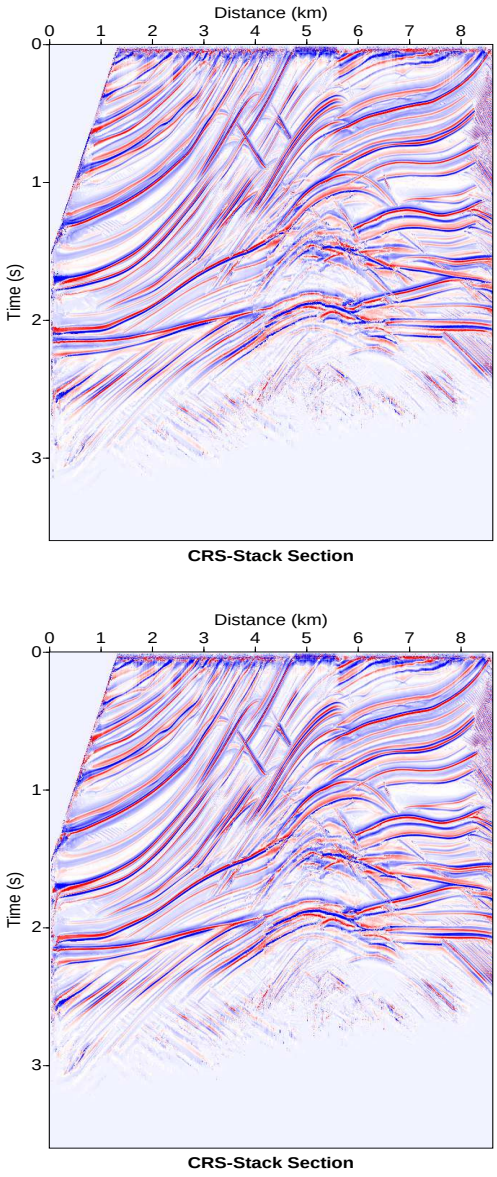

Figure 7: Stacked section before (above) and after (below) attribute smoothing with 5 points. In both sections it is seen the structural features, but with the smoothing it is not seen great relevance to the stacked section.

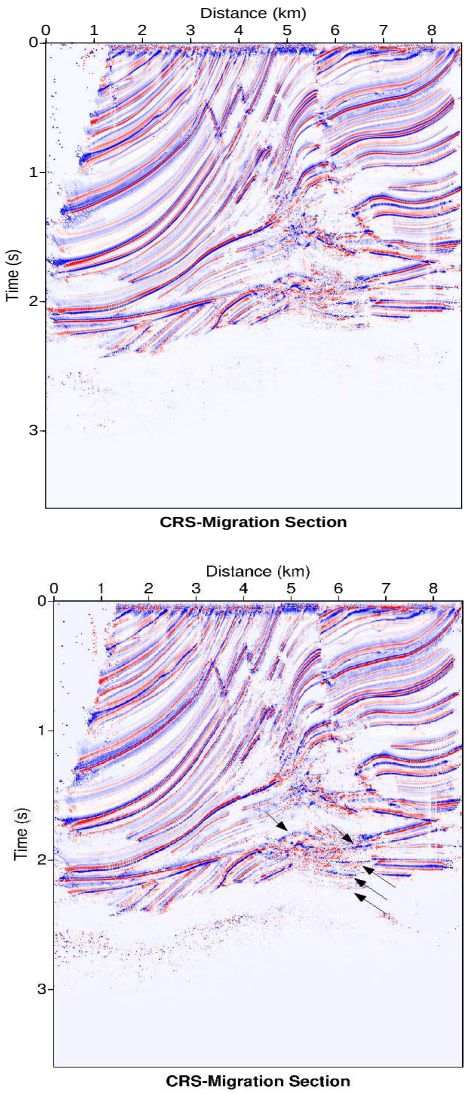

Figure 8: Migrated section before (above) and after (below) attribute smoothing with 5 points. In both sections it is seen the structural features, but with the smoothing it is possible to observe structures with better continuity in complex areas, as indicated by arrows.

The pre-processing of the jequitinhonha data consisted of defining the geometry, f and $f-k$ filtering, multiple attenuation with the SRME and RADON methods, geometrical spreading correction, and spike deconvolution. These steps have improved the signal/noise ratio, what has impoved the results of the stack and migration processes, (Nunes, 2010), according to the diagrams of figures 2 and 3. Similar to results of the syntetic data, the best advantages of smoothing the CRS attributes of the Jequitinhonha data were also related to improving the visual aspect of the migration, especially in the marked areas in figure 13, that shows better continuity of the structures.

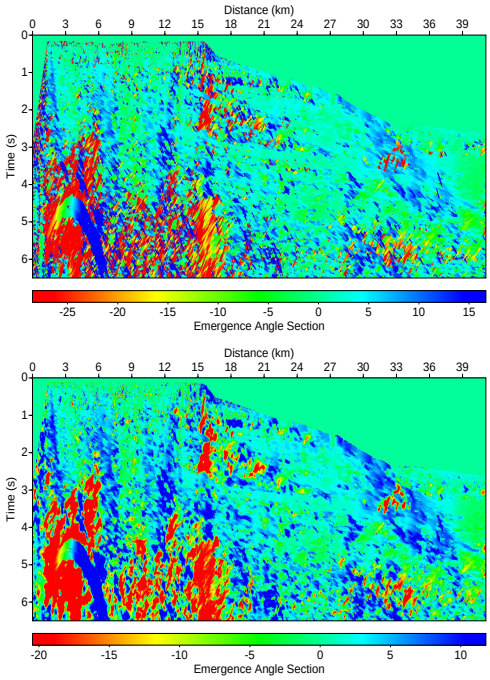

Figure 9: Emergence angle section β_0 before (above) and after (below) attribute smoothing with 10 points. In both sections it is seen the structural features, but with the smoothing it is possible to observe these structures with better signal/noise ratio.

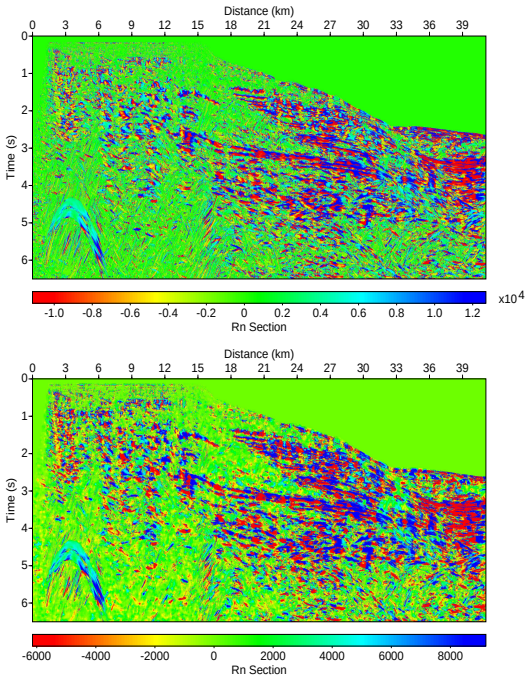

Figure 10: Curvature ray section R_N before (above) and after (below) attribute smoothing with 10 points. In both sections it is seen the structural features, but with the smoothing it is not possible to observe these structures with big changes in the signal/noise ratio.

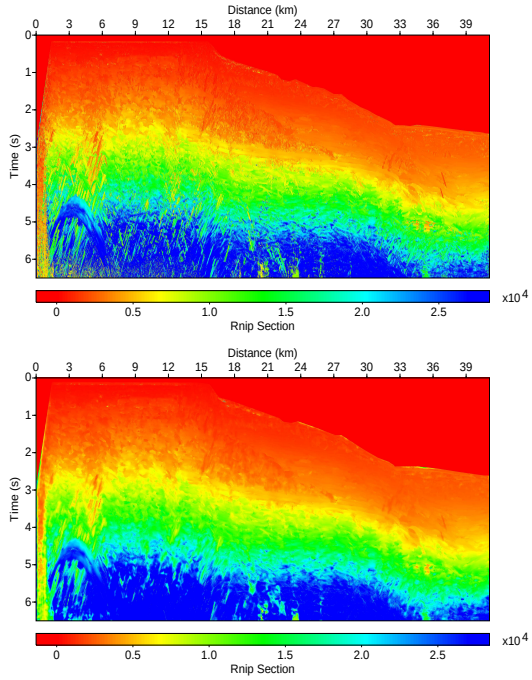

Figure 11: Curvature ray section R_{NIP} before (above) and after (below) attribute smoothing with 10 points. In both sections it is seen the structural features, but with the smoothing it is possible to observe these structures with better signal/noise ratio.

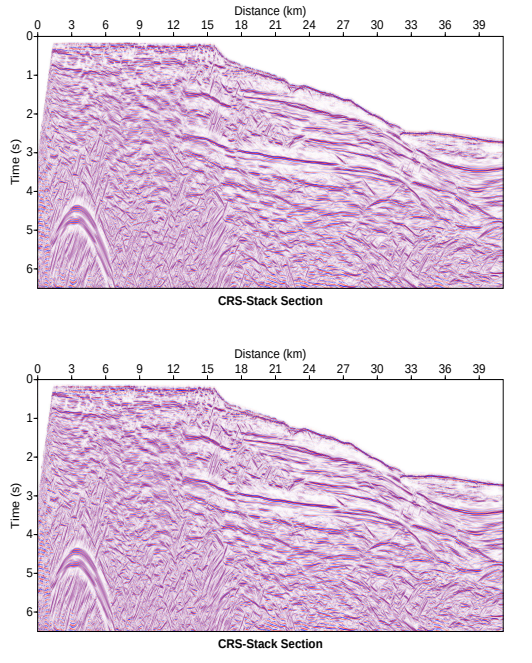

Figure 12: Stacked section before (above) and after (below) attribute smoothing with 10 points. In both sections it seen the structural features, but with the smoothing it is not seen great relevance to the stacked section.

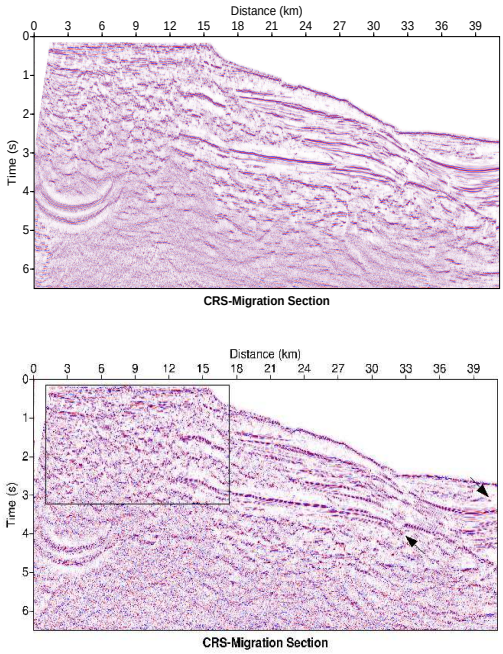

Figure 13: Migrated section before (above) and after (below) attribute smoothing with 10 points. In both sections it is seen the structural features, but with the smoothing it is possible to observe structures with better continuity in complex areas, as indicated by the arrows.

References

Mann J. 2002. Extensions and Applications of the Common-Reflection-Surface Stack Method. Dsc Thesis. Universität Karlsruhe, Germany.

Mann, J., Duveneck, E., Hertweck, T. and Jäger, C. 2003, A Seismic Reflection Imaging Workflow Based on Comom-Reflection-Surface Stack: Journal os Seismic Exploration. Number 12, p 283-295.

Mohriak, W, Szatman, P. and Anjos, S. 2008. Sal, Geologia e Tectônica - Exemplos nas Bacias Brasileiras. Beca, Brasil.

Müller, T. 1999. The Commom Reflection Surface Method - Seismic imaging without explicit knowledge of the velocity model. Dsc Thesis. Universität Karlsruhe, Germany.

Nunes, F. 2010. Processamento e Imageamento NMO/CRS de Dados Sísmicos Marinhos. Master Dissertation. Federal University of Pará, Brazil.

Acknowledgments

The authors would like to thank the Brazilian institutions UFPA (*Universidade Federal do Pará*), FINEP (*Financiadora de Estudos e Projetos*), ANP (*Agência Nacional do Petróleo*) and PETROBRAS (*Petróleo Brasileiro S/A*) for the research support, and in special to the project National Institute of Science and Technology (*Instituto Nacional de Ciência e tecnologia, INCT-GP*) do MCT/CNPq/FINEP.